Effects of Built-In Polarization and Carrier Overflow on InGaN Quantum-Well Lasers With Electronic Blocking Layers

Jun-Rong Chen, Chung-Hsien Lee, Tsung-Shine Ko, Yi-An Chang, Tien-Chang Lu, *Member, IEEE*, Hao-Chung Kuo, *Senior Member, IEEE*, Yen-Kuang Kuo, and Shing-Chung Wang, *Life Member, IEEE, Fellow, OSA*

***Abstract*—Effects of built-in polarization and carrier overflow on InGaN quantum-well lasers with a ternary AlGaN or a quaternary AlInGaN electronic blocking layer (EBL) have been numerically investigated by employing an advanced device-simulation program. The simulation results indicate that the characteristics of InGaN quantum-well lasers can be improved by using the quaternary AlInGaN EBL. When the aluminum and indium compositions in the AlInGaN EBL are appropriately designed, the built-in charge density at the interface between the InGaN barrier and the AlInGaN EBL can be reduced. Under this circumstance, the electron leakage current and the laser threshold current can obviously be decreased as compared with the laser structure with a conventional AlGaN EBL when the built-in polarization is taken into account in the calculation. Furthermore, the AlInGaN EBL also gives a higher refractive index than the AlGaN EBL, which is a benefit for a higher quantum-well optical confinement factor in laser operations.**

***Index Terms*—AlInGaN, electronic blocking layer (EBL), InGaN, numerical simulation, semiconductor lasers.**

I. Introduction

GAN-BASED semiconductor lasers and light-emitting diodes have become the most promising light sources in the applications of high-density optical storage systems and solid-state lighting [1], [2]. Although these optoelectronic devices have already been commercialized, superior operation performance and shorter emission wavelength are expected as challenges for the next-generation devices. Regarding the GaN-based semiconductor lasers, there have been lots of research groups recently devoted to realizing high-power and short-wavelength laser diodes. Kink-free blue-violet laser diodes of 100 mW were demonstrated by Asano *et al.* in 2003 [3]. Ultraviolet laser diodes with 350.9-nm-lasing wavelength were also realized by Kamiyama *et al.* in 2005 [4]. Furthermore, single-mode blue-violet laser diodes with low beam divergence and high catastrophic optical damage level were demonstrated by Ryu *et al.* in 2006 [5]. These breakthroughs make GaN-based laser diodes the potential light sources in the applications of extra-large-capacity optical storage system, biological sensing, and optical catalyst. However, the inherent problem of piezoelectric and spontaneous polarizations in c-plane GaN-based alloys is one of the most important properties which limit the development of GaN-based optoelectronic devices. The built-in polarization causes a strong deformation of the quantum wells accompanied by a strong electrostatic field. Under these circumstances, electrons and holes are separated in the quantum wells, leading to a reduction of the photon emission rate and the internal quantum efficiency [6]. Furthermore, Piprek *et al.* found that the polarization of the AlGaN electronic blocking layer (EBL) has a strong effect on the laser threshold current due to the large polarization charges [7].

Several methods have been provided to eliminate or reduce the polarization effects, such as heavy silicon (Si) doping in quantum barriers [8], nonpolar (a- and m-planes) quantum wells grown on r-plane sapphire and γ-$LiAlO_2$ [9], [10], and semipolar quantum wells grown on m-plane sapphire [11], [12]. Nevertheless, heavy Si doping in quantum barriers may induce free-carrier absorption, which results in the increase of laser threshold current. As for the nonpolar and semipolar InGaN/GaN quantum wells, high dislocation density caused by large lattice mismatch and stacking faults inhibits the related development [13]–[15].

Recently, an approach to control the electrostatic fields by using quaternary AlInGaN layers reported by Khan *et al.* could be an attractive alternative for c-plane GaN-based heterostructures since the introduction of quaternary AlInGaN layers would allow us to control both spontaneous and piezoelectric polarizations by choosing different aluminum and indium compositions [16], [17]. Since the built-in electric fields have a great impact on the properties of GaN-based laser diodes, we systematically investigate the effects of polarization on threshold current and carrier overflow using the LASer Technology Integrated Program (LASTIP) simulation program [18]. By appropriately designing the aluminum and indium compositions in AlInGaN EBLs, the built-in charge density at the interface between InGaN barrier and AlInGaN EBL can be compensated. Under this circumstance, the AlInGaN EBL can effectively inhibit the electron overflow than the conventional AlGaN EBL, and thus, the performance of the InGaN quantum-well lasers can be enhanced.

Manuscript received July 4, 2007; revised August 13, 2007. This work was supported in part by the MOE ATU program and in part by the National Science Council of the Republic of China under Contracts NSC 95-2120-M-009-008, NSC 95-2752-E-009-007-PAE, NSC 95-2221-E-009-282, and NSC 95-2112-M-018-007.

J.-R. Chen, T.-S. Ko, Y.-A. Chang, T.-C. Lu, H.-C. Kuo, and S.-C. Wang are with the Department of Photonics and Institute of Electro-Optical Engineering, National Chiao Tung University, Hsinchu 30050, Taiwan, R.O.C. (e-mail: jrchen.eo95g@nctu.edu.tw; tsko.eo93g@nctu.edu.tw; rayman0313.eo92g@nctu.edu.tw; timtclu@faculty.nctu.edu.tw; hckuo@faculty.nctu.edu.tw; scwang@cc.nctu.edu.tw).

C.-H. Lee and Y.-K. Kuo are with the Department of Physics, National Changhua University of Education, Changhua 50058, Taiwan, R.O.C. (e-mail: isaac-spider@yahoo.com.tw; ykuo@cc.ncue.edu.tw).

Digital Object Identifier 10.1109/JLT.2007.909908

0733-8724/$25.00 © 2008 IEEE

TABLE I
LAYER STRUCTURE AND ROOM-TEMPERATURE PHYSICAL PARAMETERS OF THE INGAN QUANTUM-WELL LASER UNDER STUDY (d —LAYER THICKNESS; $N_{\rm dop}$ —DOPED CARRIER DENSITY; n—REFRACTIVE INDEX AT WAVELENGTH 400 nm; κ— THERMAL CONDUCTIVITY). THE DOPED CARRIER DENSITY $N_{\rm dop}$ REPRESENTS THE ACTUAL DENSITY OF FREE CARRIERS

Parameter (unit)	d (nm)	$N_{\rm dop}$ (1/cm^3)	n	κ(W/cm K)
p-GaN (contact)	100	1×10^{18}	2.55	1.3
p-$Al_{0.07}Ga_{0.93}N$ (cladding)	1000	5×10^{17}	2.519	0.8
p-GaN (waveguide)	100	5×10^{17}	2.55	1.3
p-$Al_{0.2}Ga_{0.8}N$ (EBL)	20	5×10^{17}	2.489	0.8
i-$In_{0.035}Ga_{0.965}N$ (barrier)	5	—	2.585	0.6
i-$In_{0.1}Ga_{0.9}N$ (quantum well)	2	—	3.835	0.5
i-$In_{0.035}Ga_{0.965}N$ (barrier)	5	—	2.585	0.6
i-$In_{0.1}Ga_{0.9}N$ (quantum well)	2	—	3.835	0.5
i-$In_{0.035}Ga_{0.965}N$ (barrier)	5	—	2.585	0.6
n-GaN (waveguide)	100	1×10^{18}	2.55	1.3
n-$Al_{0.07}Ga_{0.93}N$ (cladding)	1000	1×10^{18}	2.519	0.8
n-$In_{0.1}Ga_{0.9}N$ (compliance)	100	1×10^{18}	2.835	0.5
n-GaN (substrate)	3000	1×10^{18}	2.55	1.3

II. THEORETICAL MODEL AND DEVICE STRUCTURE

In order to achieve high-performance GaN-based laser diodes, systematic and compact theoretical modeling is a necessary approach to improve the existing laser structures and to understand the internal physical processes, which provides the timely and efficient guidance toward the optimal structure design and device parameters. By performing computational simulations, we can expect the trend of device design and understand the main physical factor which limits the performance of GaN-based laser diodes.

The self-consistent LASTIP simulation program combines band structure and gain calculations with 2-D simulations of wave guiding, carrier transport, and heat flux. The carrier-transport model includes drift and diffusion of electrons and holes in devices. The built-in polarization induced by spontaneous and piezoelectric polarizations is considered at heterointerfaces of nitride-related devices. In the quantum wells, self-consistent Poisson and Schrödinger equations were recomputed at every bias point for the states of quantum-well levels and carrier distributions. The physical model of the strained InGaN quantum wells is considered in such a way that the conduction bands are assumed to be parabolic, and the valence-band structures, which include the coupling of the heavy-hole, the light-hole, and the spin-orbit split-off bands, are calculated by the 6 × 6 Hamiltonian with an envelop function approximation [19], [20]. Free-carrier gain model, including a Lorentzian broadening function with a 0.1-ps scattering time [21]–[23], is used in calculating the optical gain of the quantum wells. The calculations of carrier capture and escape from the quantum wells are considered in accordance with the model provided by Romero *et al.* [24]. More descriptions about the physical models utilized in the LASTIP simulation program can be found in [25] and [26].

In this simulation, we first assume that the InGaN laser diode is grown on an n-type GaN layer that is 3.0 μm in thickness. On top of this GaN layer are a 0.1-μm-thick n-type $In_{0.1}Ga_{0.9}N$ compliant layer and a 1.0-μm-thick n-type $Al_{0.07}Ga_{0.93}N$ cladding layer, followed by a 0.1-μm-thick n-type GaN guiding layer. The multiple-quantum-well active region consists of two 2-nm-thick $In_{0.1}Ga_{0.9}N$ quantum wells and 5-nm-thick $In_{0.035}Ga_{0.965}N$ barriers. A 20-nm-thick p-type $Al_{0.2}Ga_{0.8}N$ or p-type AlInGaN EBL is grown on top of the active region to reduce an electron leakage into the p-type GaN layer [27], [28]. Furthermore, a 0.1-μm-thick p-type GaN guiding layer and a 1.0-μm-thick p-type $Al_{0.07}Ga_{0.93}N$ cladding layer are grown. Finally, a 0.1-μm-thick p-type GaN cap layer is grown to complete the structure. The effective active region of the ridge geometry is 2 μm in width and 500 μm in length. The reflectivities of the two end mirrors are set at 20% and 50%, respectively. The doping concentrations in each layer and the detailed device structure are described in Table I.

III. MATERIAL PARAMETERS

Proper material parameters are essential to obtain correct simulation results. The material parameters of the binary semiconductors required for $k\cdot p$ calculations are taken from the paper by Vurgaftman and Meyer [29] and summarized in Table II. As for AlInGaN materials, a linear interpolation between the parameters of the relevant binary semiconductors is utilized except for the bandgap energies. For physical parameter P, the interpolation formula is [30]

$$P(\text{Al}_x\text{In}_y\text{Ga}_{1-x-y}\text{N}) = P(\text{AlN})x + P(\text{InN})y + P(\text{GaN})(1-x-y). \quad (1)$$

The AlInGaN bandgap energies can be expressed as a weighted sum of the bandgap energies of relevant ternary semiconductors with appropriate bandgap-bowing parameters. Specifically, the AlInGaN bandgap energies are calculated by the following expressions [31]:

$$E_g(\text{AlInGaN}) = \frac{xyE_g^u(\text{AlInN})+yzE_g^v(\text{InGaN})+xzE_g^w(\text{AlGaN})}{xy+yz+zx} \quad (2)$$

TABLE II
MATERIAL PARAMETERS OF THE BINARY SEMICONDUCTORS GaN, AlN, AND InN AT ROOM TEMPERATURE. ($\Delta_{\rm cr} = \Delta_1, \Delta_{\rm so} = 3\Delta_2 = 3\Delta_3$)

Parameter	Symbol (unit)	GaN	AlN	InN
Lattice constant	a_0 (Å)	3.189	3.112	3.545
Spin–orbit split energy	Δ_{so} (eV)	0.017	0.019	0.005
Crystal–field split energy	Δ_{cr} (eV)	0.010	–0.169	0.040
Hole effective mass parameter	A_1	–7.21	–3.86	–8.21
	A_2	–0.44	–0.25	–0.68
	A_3	6.68	3.58	7.57
	A_4	–3.46	–1.32	–5.23
	A_5	–3.40	–1.47	–5.11
	A_6	–4.90	–1.64	–5.96
Hydrost. deform. potential (c axis)	a_z (eV)	–4.9	–3.4	–3.5
Hydrost. deform. potential (transverse)	a_t (eV)	–11.3	–11.8	–3.5
Shear deform. potential	D_1 (eV)	–3.7	–17.1	–3.7
	D_2 (eV)	4.5	7.9	4.5
	D_3 (eV)	8.2	8.8	8.2
	D_4 (eV)	–4.1	–3.9	–4.1
Elastic stiffness constant	C_{33} (GPa)	398	373	224
Elastic stiffness constant	C_{13} (GPa)	106	108	92
Electron effective mass (c axis)	m_e^z / m_0	0.2	0.32	0.07
Electron effective mass (transverse)	m_e^t / m_0	0.2	0.30	0.07

$$E_g^u(\text{AlInN}) = uE_g(\text{InN})+(1-u)E_g(\text{AlN})-u(1-u)B(\text{AlInN}) \quad (3)$$

$$E_g^v(\text{InGaN}) = vE_g(\text{GaN})+(1-v)E_g(\text{InN})-v(1-v)B(\text{InGaN}) \quad (4)$$

$$E_g^w(\text{AlGaN}) = wE_g(\text{GaN})+(1-w)E_g(\text{AlN})-w(1-w)B(\text{AlGaN}) \quad (5)$$

$$u = \frac{1-x+y}{2}, \quad v = \frac{1-y+z}{2}, \quad w = \frac{1-x+z}{2} \quad (6)$$

where x, y , and $z = 1-x-y$ represent the compositions of aluminum, indium, and gallium in the AlInGaN material system, respectively. The bandgap-bowing parameters of AlInN, InGaN, and AlGaN are 2.5, 1.4, and 0.7 eV, respectively [29].

The built-in polarization induced due to spontaneous and piezoelectric polarizations is known to influence the performance of nitride devices. In order to consider the built-in polarization within the interfaces of nitride devices, the method developed by Fiorentini *et al.* is employed to estimate the built-in polarization, which is represented by fixed interface charges at each heterointerface. They provide explicit rules to calculate the nonlinear polarization for nitride alloys of arbitrary composition [32]. Specifically, the spontaneous polarization of ternary nitride alloys can be expressed by

$$P_{\rm sp}(\text{Al}_x\text{Ga}_{1-x}\text{N}) = -0.090x - 0.034(1-x) + 0.019x(1-x) \quad (7)$$

$$P_{\rm sp}(\text{In}_x\text{Ga}_{1-x}\text{N}) = -0.042x - 0.034(1-x) + 0.038x(1-x) \quad (8)$$

$$P_{\rm sp}(\text{Al}_x\text{In}_{1-x}\text{N}) = -0.090x - 0.042(1-x) + 0.071x(1-x). \quad (9)$$

The spontaneous polarization of the quaternary AlInGaN can be calculated in a similar way as that shown in (2). As for the piezoelectric polarization of AlInGaN, InGaN, and AlGaN, it can be calculated by the following expression:

$$P_{\rm pz}(\text{Al}_x\text{In}_y\text{Ga}_{1-x-y}\text{N}) = P_{\rm pz}(\text{AlN})x + P_{\rm pz}(\text{InN})y + P_{\rm pz}(\text{GaN})(1-x-y) \quad (10)$$

where

$$P_{\rm pz}(\text{AlN}) = -1.808\varepsilon + 5.624\varepsilon^2, \quad \text{for } \varepsilon < 0 \quad (11)$$

$$P_{\rm pz}(\text{AlN}) = -1.808\varepsilon - 7.888\varepsilon^2, \quad \text{for } \varepsilon > 0 \quad (12)$$

$$P_{\rm pz}(\text{GaN}) = -0.918\varepsilon + 9.541\varepsilon^2 \quad (13)$$

$$P_{\rm pz}(\text{InN}) = -1.373\varepsilon + 7.559\varepsilon^2 \quad (14)$$

$$\varepsilon = (a_{\rm subs} - a_L)/a_L \quad (15)$$

where $a_{\rm subs}$ and a_L are the lattice constants of the substrate and epitaxial layer, respectively. The total built-in polarization is the sum of spontaneous and piezoelectric polarizations. At an abrupt interface of a top/bottom layer heterostructure such as InGaN/GaN or AlGaN/GaN, the polarization can decrease or increase within a bilayer, causing a fixed polarization charge density σ defined by [33]

$$\sigma(P_{\rm sp}+P_{\rm pz}) = P(\text{bottom}) - P(\text{top}) = [P_{\rm sp}(\text{bottom})+P_{\rm pz}(\text{bottom})] - [P_{\rm sp}(\text{top})+P_{\rm pz}(\text{top})] \quad (16)$$

TABLE III
NET SURFACE CHARGE DENSITY AT EACH INTERFACE OF THE InGaN LASER DIODE

Interface	Built-in charge density
$Al_{0.07}Ga_{0.93}N/GaN$	$+2.86\times10^{12}$ cm^{-2}
$GaN/Al_{0.2}Ga_{0.8}N$	-8.82×10^{12} cm^{-2}
$Al_{0.2}Ga_{0.8}N/In_{0.035}Ga_{0.965}N$	$+1.20\times10^{13}$ cm^{-2}
$In_{0.035}Ga_{0.965}N/In_{0.1}Ga_{0.9}N$	$+6.46\times10^{12}$ cm^{-2}
$In_{0.1}Ga_{0.9}N/In_{0.035}Ga_{0.965}N$	-6.46×10^{12} cm^{-2}
$In_{0.035}Ga_{0.965}N/GaN$	-3.19×10^{12} cm^{-2}
$GaN/Al_{0.07}Ga_{0.93}N$	-2.86×10^{12} cm^{-2}

For the InGaN quantum-well lasers under study, the net surface charges at all interfaces are calculated and listed in Table III . Although the interface charges can be obtained by this theoretical model, experimental investigations often find a weaker built-in polarization than that predicted by theoretical calculation. It is mainly attributed to partial compensation of the built-in polarization by defect and interface charges [34]. Typical reported experimental values are 20%, 50%, or 80% smaller than the theoretically calculated values [35]–[37]. As a result, 0% to 40% of the theoretical polarization values are used in our simulation to study the effects of built-in polarization on the laser performance.

The thermal conductivities of nitride compounds listed in Table I are obtained from the values of binary GaN, AlN, and InN by considering the impact of alloy and the interface scattering of phonons. In our simulation, the thermal conductivities of GaN, AlN, and InN are 1.3, 2.85, and 0.45 W/cm · K, respectively [25]. As for the parameter of refractive index, Adachi model is employed to calculate the refractive-index values in each layer listed in Table I as well [38]. Band offset ratio, which is defined as the ratio between the conduction-band offset ΔE_c and the valence-band offset ΔE_v of the InGaN/InGaN quantum well, is assumed to be 0.7/0.3 based on the published works [39], [40].

IV. SIMULATION RESULTS AND DISCUSSION

The energy band diagram of the InGaN/InGaN double quantum-well active region with a conventional $Al_{0.2}Ga_{0.8}N$ EBL at 500-mA injection current is shown in Fig. 1. Since the threshold current of the InGaN quantum-well laser with an $Al_{0.2}Ga_{0.8}N$ EBL is larger than 300 mA when the 40% polarization is considered in the calculation, we choose the injection current at 500 mA in order to analyze the internal physical processes of this laser diode above threshold and at higher operation current. In Fig. 1, the dashed line is calculated without considering the interface charge density, and the solid line is calculated with 40% interface charge density listed in Table III. It can be found that the conduction and valence bands are strongly deformed when the built-in polarization is assumed to be 40% of the theoretically calculated values. Although the injection current is 500 mA, the built-in polarization field still

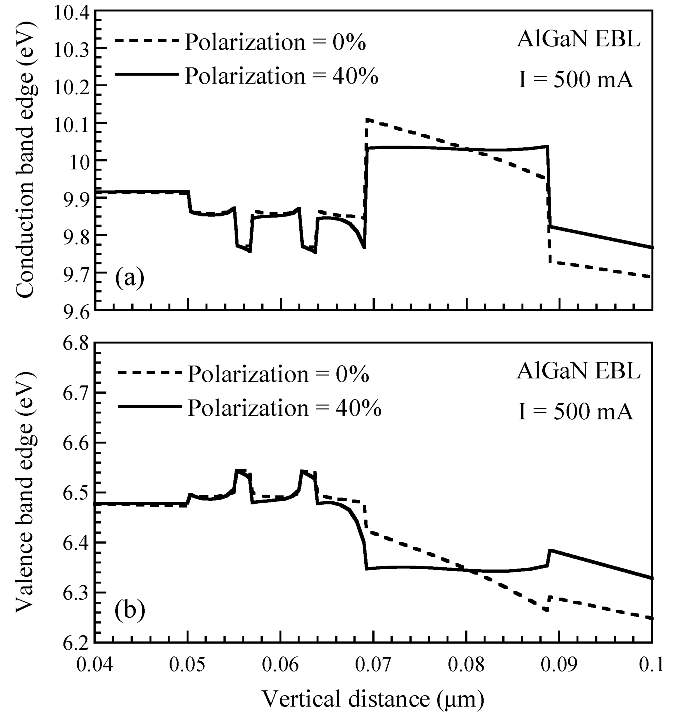

Fig. 1. Energy band diagram of the InGaN/InGaN double quantum-well active region at 500-mA injection current. (a) Conduction bands for 0% (dashed line) and 40% (solid line) polarizations. (b) Valence bands for 0% (dashed line) and 40% (solid line) polarizations.

significantly deforms the energy band diagram in this operation current [18]. It is noteworthy that the energy barrier height created by $Al_{0.2}Ga_{0.8}N$ EBL is substantially reduced by the high density of positive polarization charges at the interface between the InGaN barrier layer and the AlGaN EBL. Under this condition, the electrons are attracted by a Coulomb force and accumulate at this interface, which leads to a strong band bending. Consequently, the increase of laser threshold current will be expected due to the enhanced electron carrier leakage from the active layer to the p-type cladding layer. The leakage current results in an increased nonradiative recombination and lowers the internal quantum efficiency particularly for laser diodes operated at high injection level or at high operation temperature. The vertical profiles of electron-concentration distribution and conduction-band edge in the active region at 500-mA injection current are shown in Fig. 2 for laser structure with $Al_{0.2}Ga_{0.8}N$ EBLs. We also compare different polarization percentage values, i.e., without polarization [Fig. 2(a)] and with 40% polarization [Fig. 2(b)]. It is obviously observed that a large number of electrons are attracted by the positive polarization charges and accumulate at the AlGaN EBL in the case of 40% polarization [Fig. 2(b)]. This condition makes a strong band bending at the InGaN/AlGaN interface, which lowers the AlGaN energy barrier relative to the electron quasi-Fermi level from 180 to 90 meV when the polarization percentage value changes from 0% to 40%. Although the energy barrier can be higher by increasing the p-type doping concentration in the AlGaN EBL, it is difficult to achieve a high p-type conductivity

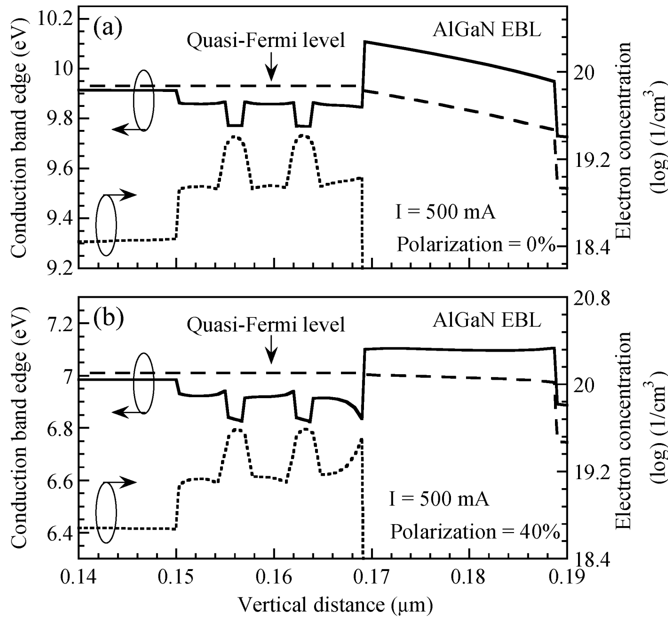

Fig. 2. Vertical profiles of electron-concentration distribution and conduction-band edge in the active region of the laser structure with AlGaN EBL at 500-mA injection current. (a) 0% polarization. (b) 40% polarization.

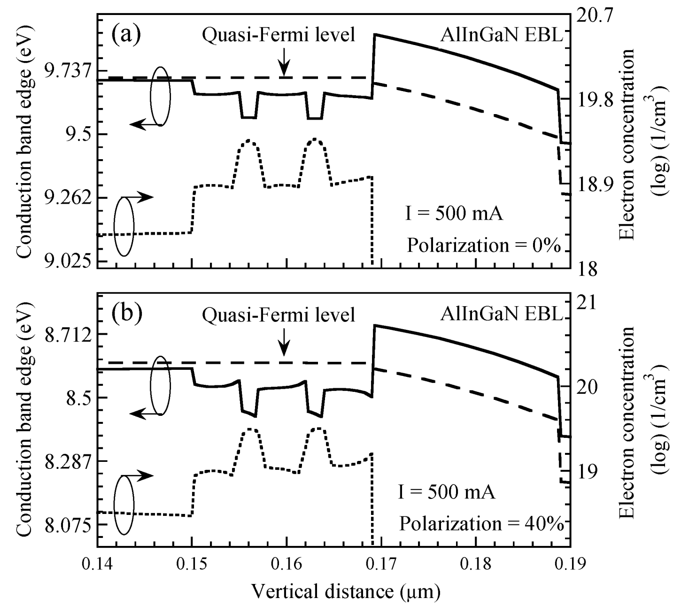

Fig. 3. Vertical profiles of electron-concentration distribution and conduction-band edge in the active region of the laser structure with AlInGaN EBL at 500-mA injection current. (a) 0% polarization. (b) 40% polarization.

in the p-type AlGaN alloys due to the high activation energy of Mg dopants [41].

In order to reduce the high density of interface charges at the InGaN/AlGaN interface, the quaternary AlInGaN EBL could be used to replace the conventional ternary $Al_{0.2}Ga_{0.8}N$ EBL. Since it is assumed that the laser structures are grown on GaN bulk, the strains of AlGaN and InGaN epitaxial layers are tensile and compressive, respectively, which makes the directions of the piezoelectric polarization of AlGaN and InGaN opposite. Therefore, by employing appropriate aluminum and indium compositions in the AlInGaN EBL, it was found that the built-in charge density at the interface between the $In_{0.035}Ga_{0.965}N$ barrier and AlInGaN EBL can be compensated according to the results of theoretical calculation. The aluminum and indium compositions are determined by fixing a specific aluminum composition and varying the indium composition to find the minimum interface charge density. When different aluminum compositions are chosen, there are corresponding indium compositions which make the InGaN/AlInGaN interface charge density minimum. Therefore, several different aluminum and indium compositions can reach this requirement. For comparison purpose, $Al_{0.25}In_{0.144}Ga_{0.606}N$ is chosen to be the quaternary EBL in this paper because its energy bandgap is nearly identical to that of the original $Al_{0.2}Ga_{0.8}N$ EBL after considering the strain-induced bandgap variation in both EBLs. The interface charge density between the $In_{0.035}Ga_{0.965}N$ barrier and the $Al_{0.25}In_{0.144}Ga_{0.606}N$ EBL is -1.7×10^{10} cm^{-2}, which is calculated by (7) –(14). This value is dramatically reduced as compared with that of the conventional $Al_{0.2}Ga_{0.8}N$ EBL.

Fig. 3 shows the vertical profiles of the electron-concentration distribution and conduction-band edge without polarization [Fig. 3(a)] and with 40% polarization [Fig. 3(b)] in the active region at 500-mA injection current for laser structure with AlInGaN EBLs. The electron-concentration distributions and conduction-band diagrams of the laser structures with AlGaN and AlInGaN EBLs are nearly identical when the built-in polarization is not taken into account [Figs. 2(a) and 3(a)]. Therefore, we expect that the laser performance will be similar, which is shown in later simulation results. On the contrary, in the case of considering the 40% built-in polarization, the conduction band near the interface of the InGaN barrier and the AlInGaN EBL is only slightly deformed due to the reduced density of the polarization charges. Relatively small electron accumulation at the AlInGaN EBL is observed, and the AlInGaN energy barrier relative to the electron quasi-Fermi level is about 130 meV for 40% polarization.

Fig. 4 shows the vertical electron current profile within the active regions of laser structures with AlGaN and AlInGaN EBLs at 500-mA injection current. The positions of the two quantum wells are marked with gray areas. The left-hand side of the figure is the n-side of the device. The electron current is injected from the n-type layers into the quantum wells and recombines with holes in the quantum wells. Therefore, the electron current density is reduced in the quantum wells. An electron current, which overflows through the quantum wells, is viewed as the leakage current. In Fig. 4(a), the vertical electron current profile of the laser diodes with different EBLs is nearly identical when the built-in polarization is not considered. As for the calculation results with consideration of the 40% polarization, the electron current profiles of these two laser structures are obviously different [Fig. 4(b)]. It is found that the electron leakage current of the laser structure with the AlGaN EBL is relatively larger than that of the laser structure with the AlInGaN EBL due to the lower barrier height at the InGaN/AlGaN interface. Fig. 5 shows the stimulated recombination rate for laser structures with

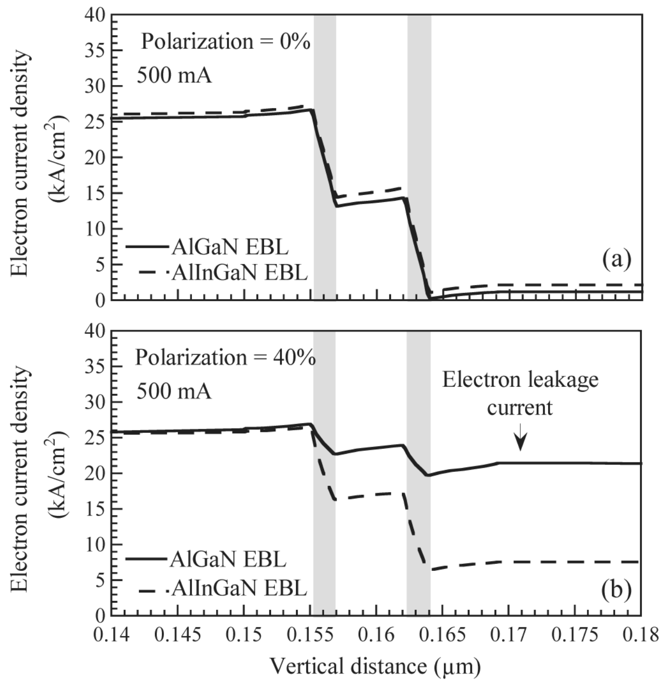

Fig. 4. Vertical electron current profile for laser structures with AlGaN and AlInGaN EBLs at 500-mA injection current. (a) 0% polarization. (b) 40% polarization.

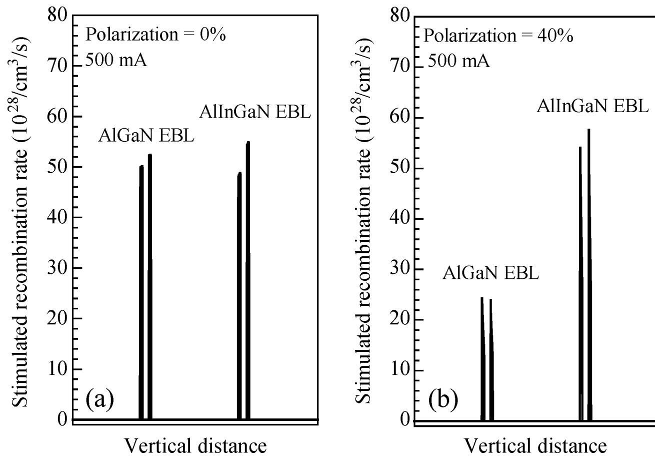

Fig. 5. Stimulated recombination rate for laser structures with AlGaN and AlInGaN EBLs at 500-mA injection current. (a) 0% polarization. (b) 40% polarization.

AlGaN and AlInGaN EBLs at 500-mA injection current when the polarization values are considered with 0% [Fig. 5(a)] and 40% [Fig. 5(b)], respectively. In Fig. 5(a), the stimulated recombination rate of laser diodes with different EBLs is nearly identical when the built-in polarization is not considered. However, by taking the 40% polarization into account, the stimulated recombination rate of the laser diode with the AlGaN EBL is relatively lower than that of the laser diode with the AlInGaN EBL, as shown in Fig. 5(b). Therefore, the large electron leakage current induced by the lower barrier height at the InGaN/AlGaN interface of the laser diode with the AlGaN EBL lowers the stimulated recombination rate in the quantum wells. By employing

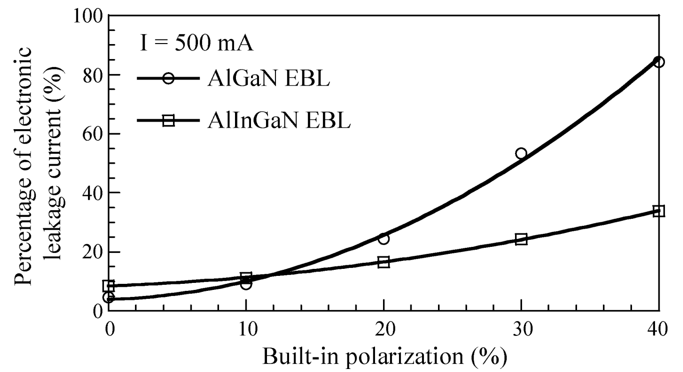

Fig. 6. Percentage of electron leakage current versus built-in polarization charges for laser diodes with AlGaN and AlInGaN EBLs.

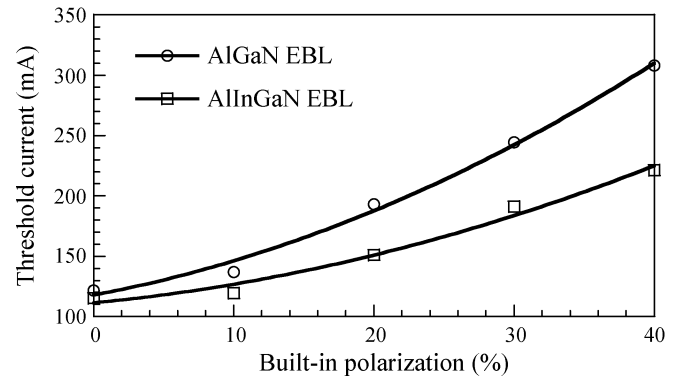

Fig. 7. Laser threshold current versus percentage of built-in polarization charges for laser diodes with AlGaN and AlInGaN EBLs.

the AlInGaN EBL, the electron leakage current obviously decreases, and the stimulated recombination rate can significantly be enhanced.

In order to further understand the effects of the built-in polarization on the electron leakage current, the percentage of electron leakage current versus built-in polarization charges for laser diodes with AlGaN and AlInGaN EBLs is shown in Fig. 6. The percentage of the electron leakage current is defined as the ratio of the electron current overflowed to the p-type layer to that injected into the active region of the laser diodes. Since the effective energy barrier provided by the AlGaN EBL is reduced with increasing polarization charges, the percentage of the electron leakage current increases with the amount of polarization charges as well. The difference of the percentage of the electron leakage between the laser structures with AlGaN and AlInGaN EBLs becomes more obvious with increasing polarization charges. In the case of no polarization, the electron leakage of the laser structure with the AlInGaN EBL is slightly larger than that of the laser structure with the AlGaN EBL. It is attributed to the difference of conduction-band offset between the InGaN barrier layer and the EBLs. Note that the energy barriers provided by the AlGaN and AlInGaN EBLs are 264 and 242 meV, respectively. Although the same band offset ratio is considered in our simulation, the conduction- and valence-band edges will be modified by strain effects. Therefore, after taking this effect on the bandgap of the EBL into account, the energy barrier created by the AlInGaN EBL is lower, which leads to a

slightly larger electron leakage when the built-in polarization is omitted.

Fig. 7 shows the laser threshold current versus built-in polarization charges for the laser structures with the AlGaN and AlInGaN EBLs. In the condition of no polarization, the threshold current of the laser structure with the AlInGaN EBL is slightly smaller than that of the laser structure with the AlGaN EBL even though the electron leakage is larger, as shown in Fig. 6. To understand this simulation result, we compare the quantum-well optical confinement factors of the two laser structures. The calculated results show that the quantum-well optical confinement factor of the laser structure with the AlInGaN EBL is larger than that of the laser structure with the AlGaN EBL due to the higher refractive index of the AlInGaN layer. The values of the quantum-well optical confinement factors are 1.2% and 1.6% for laser structures with AlGaN and AlInGaN EBLs, respectively. Furthermore, the threshold current becomes higher with increasing built-in polarization, owing to the increase of electron leakage current. The improvement of the threshold current for InGaN quantum-well laser with AlInGaN EBL is more obvious for high level of built-in polarization. Therefore, according to the simulation results, the InGaN quantum-well lasers using a quaternary AlInGaN EBL can effectively inhibit the electron leakage current and lower the threshold current when the built-in polarization is taken into account in our simulation.

V. Conclusion

In conclusion, the built-in polarization of the EBL plays an important role in the InGaN quantum-well lasers. The large amount of polarization charges at the interface between the InGaN barrier layer and the conventional AlGaN EBL are found to dramatically enhance the electron leakage and cause an additional increase in the threshold current. In order to reduce this polarization effect, the InGaN quantum-well lasers with AlGaN and AlInGaN EBLs are systematically investigated in this paper. By comparing the effects of the electron leakage and the threshold current of the laser structures with different EBLs, the simulation results suggest that the laser performance can be markedly improved by employing the quaternary AlInGaN EBL. In the meantime, the simulation results also show that the quantum-well optical confinement factor increases for the laser structure with an AlInGaN EBL due to its higher refractive index when compared to the conventional AlGaN EBL.

References

[1] S. Nakamura and G. Fasol, *The Blue Laser Diode*. Berlin, Germany: Springer-Verlag, 1997.

[2] D. A. Steigerwald, J. C. Bhat, D. Collins, R. M. Fletcher, M. O. Holcomb, M. J. Ludowise, P. S. Martin, and S. L. Rudaz, "Illumination with solid state lighting technology," *IEEE J. Sel. Topics Quantum Electron.*, vol. 8, no. 2, pp. 310–320, Mar./Apr. 2002.

[3] T. Asano, T. Tojyo, T. Mizuno, M. Takeya, S. Ikeda, K. Shibuya, T. Hino, S. Uchida, and M. Ikeda, "100-mW kink-free blue-violet laser diodes with low aspect ratio," *IEEE J. Quantum Electron.*, vol. 39, no. 1, pp. 135–140, Jan. 2003.

[4] S. Kamiyama, K. Iida, T. Kawashima, H. Kasugai, S. Mishima, A. Honshio, Y. Miyake, M. Iwaya, H. Amano, and I. Akasaki, "UV laser diode with 350.9-nm-lasing wavelength grown by hetero-epitaxial-lateral overgrowth technology," *IEEE J. Sel. Topics Quantum Electron.*, vol. 11, no. 5, pp. 1069–1073, Sep./Oct. 2005.

[5] H. Y. Ryu, H. Ha, S. N. Lee, K. K. Choi, T. Jang, J. K. Son, J. H. Chae, S. H. Chae, H. S. Paek, Y. J. Sung, T. Sakong, H. G. Kim, K. S. Kim, Y. H. Kim, O. H. Nam, and Y. J. Park, "Single-mode blue-violet laser diodes with low beam divergence and high COD level," *IEEE Photon. Technol. Lett.*, vol. 18, no. 9, pp. 1001–1003, May 2006.

[6] L. H. Peng, C. W. Chuang, and L. H. Lou, "Piezoelectric effects in the optical properties of strained InGaN quantum wells," *Appl. Phys. Lett.*, vol. 74, no. 6, pp. 795–797, Feb. 1999.

[7] J. Piprek, R. Farrell, S. DenBaars, and S. Nakamura, "Effects of built-in polarization on InGaN-GaN vertical-cavity surface-emitting lasers ," *IEEE Photon. Technol. Lett.*, vol. 18, no. 1, pp. 7–9, Jan. 2006.

[8] G. Franssen, T. Suski, P. Perlin, R. Bohdan, A. Bercha, W. Trzeciakowski, I. Makarowa, P. Prystawko, M. Leszczyñski, I. Grzegory, S. Porowski, and S. Kokenyesi, "Fully-screened polarization-induced electric fields in blue/violet InGaN/GaN light-emitting devices grown on bulk GaN," *Appl. Phys. Lett.*, vol. 87, no. 4, p. 041109, Jul. 2005.

[9] M. D. Craven, S. H. Lim, F. Wu, J. S. Speck, and S. P. DenBaars, "Structural characterization of nonpolar $(11\overline{2}0)$ a-plane GaN thin films grown on $(1\overline{1}02)$ r-plane sapphire," *Appl. Phys. Lett.*, vol. 81, no. 3, pp. 469–471, Jul. 2002.

[10] P. Waltereit, O. Brandt, A. Trampert, H. T. Grahn, J. Menniger, M. Ramsteiner, M. Reiche, and K. H. Ploog, "Nitride semiconductors free of electrostatic fields for efficient white light-emitting diodes ," *Nature*, vol. 406, no. 6798, pp. 865–868, Aug. 2000.

[11] X. Ni, Ü. Özgür, A. A. Baski, H. Morkoç, L. Zhou, D. J. Smith, and C. A. Tran, "Epitaxial lateral overgrowth of $(11\overline{2}2)$ semipolar GaN on $(1\overline{1}00)$ m-plane sapphire by metalorganic chemical vapor deposition," *Appl. Phys. Lett.*, vol. 90, no. 18, p. 182 109, Apr. 2007.

[12] R. Sharma, P. M. Pattison, H. Masui, R. M. Farrell, T. J. Baker, B. A. Haskell, F. Wu, S. P. DenBaars, J. S. Speck, and S. Nakamura, "Demonstration of a semipolar $(10\overline{1}\overline{3})$ InGaN/GaN green light emitting diode," *Appl. Phys. Lett.*, vol. 87, no. 23, p. 231 110, Dec. 2005.

[13] H. Yu, L. K. Lee, T. Jung, and P. C. Ku, "Photoluminescence study of semipolar $\{10\overline{1}1\}$ InGaN/GaN multiple quantum wells grown by selective area epitaxy," *Appl. Phys. Lett.*, vol. 90, no. 14, p. 141 906, Apr. 2007.

[14] T. Paskova, R. Kroeger, S. Figge, D. Hommel, V. Darakchieva, B. Monemar, E. Preble, A. Hanser, N. M. Williams, and M. Tutor, "High-quality bulk a-plane GaN sliced from boules in comparison to heteroepitaxially grown thick films on r-plane sapphire," *Appl. Phys. Lett.*, vol. 89, no. 5, p. 051 914, Jul. 2006.

[15] A. Chakraborty, K. C. Kim, F. Wu, J. S. Speck, S. P. DenBaars, and U. K. Mishra, "Defect reduction in nonpolar a-plane GaN films using *in situ* SiN_x nanomask," *Appl. Phys. Lett.*, vol. 89, no. 4, p. 041903, Jul. 2006.

[16] M. A. Khan, J. W. Yang, G. Simin, R. Gaska, M. S. Shur, H.-C. Loye, G. Tamulaitis, A. Zukauskas, D. J. Smith, D. Chandrasekhar, and R. Bicknell-Tassius, "Lattice and energy band engineering in AlInGaN/GaN heterostructures," *Appl. Phys. Lett.*, vol. 76, no. 9, pp. 1161–1163, Feb. 2000.

[17] J. Zhang, J. Yang, G. Simin, M. Shatalov, M. A. Khan, M. S. Shur, and R. Gaska, "Enhanced luminescence in InGaN multiple quantum wells with quaternary AlInGaN barriers ," *Appl. Phys. Lett.*, vol. 77, no. 17, pp. 2668–2670, Oct. 2000.

[18] LASTIP Version 2005.11. Burnaby, BC, Canada, Crosslight Softw., 2005. Burnaby, BC, Canada.

[19] S. L. Chuang and C. S. Chang, "$k \cdot p$ method for strained wurtzite semiconductors ," *Phys. Rev. B, Condens. Matter*, vol. 54, no. 4, pp. 2491–2504, Jul. 1996.

[20] S. L. Chuang and C. S. Chang, "Effective-mass Hamiltonian for strained wurtzite GaN and analytical solutions," *Appl. Phys. Lett.*, vol. 68, no. 12, pp. 1657–1659, Mar. 1996.

[21] S. L. Chuang, "Optical gain of strained wurtzite GaN quantum-well lasers," *IEEE J. Quantum Electron.*, vol. 32, no. 10, pp. 1791–1800, Oct. 1996.

[22] Y. C. Yeo, T. C. Chong, M.-F. Li, and W. J. Fan, "Electronic band structures and optical gain spectra of strained wurtzite GaN-$Al_xGa_{1-x}N$ quantum-well lasers," *IEEE J. Quantum Electron.*, vol. 34, no. 3, pp. 526–534, Mar. 1998.

[23] Y. C. Yeo, T. C. Chong, M. F. Li, and W. J. Fan, "Analysis of optical gain and threshold current density of wurtzite InGaN/GaN/AlGaN quantum well lasers," *J. Appl. Phys.*, vol. 84, no. 4, pp. 1813–1819, Aug. 1998.

[24] B. Romero, J. Arias, I. Esquivias, and M. Cada, "Simple model for calculating the ratio of the carrier capture and escape times in quantum-well lasers," *Appl. Phys. Lett.*, vol. 76, no. 12, pp. 1504–1506, Mar. 2000.

[25] J. Piprek, *Semiconductor Optoelectronic Devices: Introduction to Physics and Simulation*. San Diego, CA: Academic, 2003.

[26] *"LASTIP User's Manual Version 2005.11,"* 1st ed. Crosslight Softw., Burnaby, BC, Canada, 2005.

[27] K. Domen, R. Soejima, A. Kuramata, and T. Tanahashi, "Electron overflow to the AlGaN p-cladding layer in InGaN/GaN/AlGaN MQW laser diodes ," *MRS Internet J. Nitride Semicond. Res.*, vol. 3, no. 2, pp. 2–7, 1998.

[28] Y.-K. Kuo and Y.-A. Chang, "Effects of electronic current overflow and inhomogeneous carrier distribution on InGaN quantum-well laser performance," *IEEE J. Quantum Electron.*, vol. 40, no. 5, pp. 437–444, May 2004.

[29] I. Vurgaftman and J. R. Meyer, "Band parameters for nitrogen-containing semiconductors," *J. Appl. Phys.*, vol. 94, no. 6, pp. 3675–3691, Sep. 2003.

[30] J. Minch, S. H. Park, T. Keating, and S. L. Chuang, "Theory and experiment of $In_{1-x}Ga_xAs_yP_{1-y}$ and $In_{1-x-y}Ga_xAl_yAs$ long-wavelength strained quantum-well lasers," *IEEE J. Quantum Electron.*, vol. 35, no. 5, pp. 771–782, May 1999.

[31] I. Vurgaftman, J. R. Meyer, and L. R. Ram-Mohan, "Band parameters for III–V compound semiconductors and their alloys," *J. Appl. Phys.*, vol. 89, no. 11, pp. 5815–5875, Jun. 2001.

[32] V. Fiorentini, F. Bernardini, and O. Ambacher, "Evidence for nonlinear macroscopic polarization in III–V nitride alloy heterostructures ," *Appl. Phys. Lett.*, vol. 80, no. 7, pp. 1204–1206, Feb. 2002.

[33] O. Ambacher, B. Foutz, J. Smart, J. R. Shealy, N. G. Weimann, K. Chu, M. Murphy, A. J. Sierakowski, W. J. Schaff, L. F. Eastman, R. Dimitrov, A. Mitchell, and M. Stutzmann, "Two dimensional electron gases induced by spontaneous and piezoelectric polarization in undoped and doped AlGaN/GaN heterostructures," *J. Appl. Phys.*, vol. 87, no. 1, pp. 334–344, Jan. 2000.

[34] J. P. Ibbetson, P. T. Fini, K. D. Ness, S. P. DenBaars, J. S. Speck, and U. K. Mishra, "Polarization effects, surface states, and the source of electrons in AlGaN/GaN heterostructure field effect transistors," *Appl. Phys. Lett.*, vol. 77, no. 2, pp. 250–252, Jul. 2000.

[35] S. F. Chichibu, A. C. Abare, M. S. Minsky, S. Keller, S. B. Fleischer, J. E. Bowers, E. Hu, U. K. Mishra, L. A. Coldren, S. P. DenBaars, and T. Sota, "Effective band gap inhomogeneity and piezoelectric field in InGaN/GaN multiquantum well structures ," *Appl. Phys. Lett.*, vol. 73, no. 14, pp. 2006–2008, Oct. 1998.

[36] H. Zhang, E. J. Miller, E. T. Yu, C. Poblenz, and J. S. Speck, "Measurement of polarization charge and conduction-band offset at $In_xGa_{1-x}N$/GaN heterojunction interfaces," *Appl. Phys. Lett.*, vol. 84, no. 23, pp. 4644–4646, Jul. 2004.

[37] F. Renner, P. Kiesel, G. H. Dõhler, M. Kneissl, C. G. Van de Walle, and N. M. Johnson, "Quantitative analysis of the polarization fields and absorption changes in InGaN/GaN quantum wells with electroabsorption spectroscopy," *Appl. Phys. Lett.*, vol. 81, no. 3, pp. 490–492, Jul. 2002.

[38] T. Peng and J. Piprek, "Refractive index of AlGaInN alloys," *Electron. Lett.*, vol. 32, no. 24, pp. 2285–2286, Nov. 1996.

[39] S.-H. Wei and A. Zunger, "Valence band splittings and band offsets of AlN, GaN, and InN," *Appl. Phys. Lett.*, vol. 69, no. 18, pp. 2719–2721, Oct. 1996.

[40] Y.-K. Kuo, B.-T. Liou, M.-L. Chen, S.-H. Yen, and C.-Y. Lin, "Effect of band-offset ratio on analysis of violet-blue InGaN laser characteristics," *Opt. Commun.*, vol. 231, no. 1–6, pp. 395–402, Feb. 2004.

[41] J. Li, T. N. Oder, M. L. Nakarmi, J. Y. Lin, and H. X. Jiang, "Optical and electrical properties of Mg-doped p-type $Al_xGa_{1-x}N$," *Appl. Phys. Lett.*, vol. 80, no. 7, pp. 1210–1212, Feb. 2002.

Jun-Rong Chen was born in Taichung, Taiwan, R.O.C., on October 23, 1980. He received the B.S. degree in physics from the National Changhua University of Education (NCUE), Changhua, Taiwan, in 2004 and the M.S. degree in optoelectronics from the Institute of Photonics, NCUE, in 2006. He is currently working toward the Ph.D. degree in the Department of Photonics and Institute of Electro-Optical Engineering, National Chiao Tung University (NCTU), Hsinchu, Taiwan.

He joined the Semiconductor Laser Technology Laboratory, NCTU, in 2006, where he was engaged in research on III-V semiconductor materials for light-emitting diodes and on semiconductor lasers under the instruction of Prof. Tien-Chang Lu, Prof. Hao-Chung Kuo, and Prof. Shing-Chung Wang. His recent research interests include III-nitride semiconductor lasers, epitaxial growth of III-nitride materials, and numerical simulation of III-V optoelectronic devices.

Chung-Hsien Lee was born in Taiwan, R.O.C. He received the B.S. degree in physics from Tamkang University, Taipei, Taiwan, in 2005. He is currently working toward the M.S. degree in optoelectronics at the Institute of Photonics, National Changhua University of Education (NCUE), Changhua, Taiwan.

He has been with the Laboratory of Lasers and Optical Semiconductors, NCUE, since 2005, where he has been engaged in research on III-V semiconductor materials for light-emitting diodes and on semiconductor lasers under the instruction of Prof. Yen-Kuang Kuo. His recent research interests include III-nitride semiconductor lasers, vertical-cavity surface-emitting lasers, and light-emitting diodes.

Tsung-Shine Ko was born in Tainan, Taiwan, R.O.C., in 1978. He received the B.S. degree in physics from the National Changhua University, Changhua, Taiwan, in 2001 and the M.S. degree in atomic science from the National Tsing Hau University, Hsinchu, Taiwan, in 2004. Since 2004, he has been working toward the Ph.D. degree at the Institute of Electro-Optical Engineering, National Chiao Tung University, Hsinchu.

After he received the B.S. degree in 2001, he was a Practice Teacher for one year with. He was engaged in research on the design of masks for extreme ultraviolet, the synthesis of gold nanoparticles, and the growth of Si/Ge nanostructures under the instruction of Dr. J. Shieh, Prof. H. L. Chen, and Prof. T. C. Chu. His current research interests include the fabrication of nanostructure oxide materials and the epitaxial growth of nonpolar GaN-based materials under the instruction of Prof. T. C. Lu, Prof. H. C. Kuo, and Prof. S. C. Wang.

Yi-An Chang was born in Taipei, Taiwan, R.O.C., on March 13, 1978. He received the B.S. and M.S. degrees in physics from the National Changhua University of Education (NCUE), Changhua, Taiwan, in 2001 and 2003, respectively. He is currently working toward the Ph.D. degree at the Institute of Electro-optical Engineering, National Chiao Tung University, Hsinchu, Taiwan.

He was with the Laboratory of Lasers and Optical Semiconductors, NCUE, in 2000, where he was engaged in research on passive Q-switching with solid-state saturable absorbers and III-nitride semiconductor materials for light-emitting diodes and semiconductor lasers under the instruction of Prof. Yen-Kuang Kuo. His current research interests include III-nitride and InGaAsN semiconductor devices and infrared vertical-cavity surface-emitting lasers under the instruction of Prof. Hao-Chung Kuo and Prof. Shing-Chung Wang.

Tien-Chang Lu (M'07) received the B.S. degree in electrical engineering from the National Taiwan University, Taipei, Taiwan, R.O.C., in 1995, the M.S. degree in electrical engineering from the University of Southern California, Los Angeles, in 1998, and the Ph.D. degree in electrical engineering and computer science from the National Chiao Tung University, Hsinchu, Taiwan, in 2004.

He was with the Union Optronics Corporation as a Manager of Epitaxy Department in 2004. Since August 2005, he has been with the National Chiao Tung University as a member of the faculty in the Department of Photonics. His research work included the design, epitaxial growth, process, and characterization of optoelectronic devices such as Fabry–Perot-type semiconductor lasers, vertical-cavity surface-emitting lasers, resonant-cavity light-emitting diodes (LEDs), wafer-fused flip-chip LEDs, solar cells, etc. He has been engaged in

the low-pressure MOCVD epitaxial technique associated with various material systems including InGaAlAs, InGaAsP, AlGaAs, InGaAlP, and InGaAlN as well as the corresponding process skills. He is also interested in the structure design and simulations for optoelectronic devices using computer-aided software.

Hao-Chung Kuo (S'98–M'99–SM'06) received the B.S. degree in physics from the National Taiwan University, Taipei, Taiwan, R.O.C., in 1990, the M.S. degree in electrical and computer engineering from Rutgers University, Camden, NJ, in 1995, and the Ph.D. degree in electrical and computer engineering from the University of Illinois at Urbana–Champaign in 1999.

He has an extensive professional career both in research and industrial research institutions, which includes as follows: Research Consultant with Lucent Technologies, Bell Lab, Holmdel, NJ, (from 1995 to 1997), R&D Engineer with the Fiber-optics Division, Agilent Technologies (from 1999 to 2001), and R&D Manager with LuxNet Corporation (from 2001 to 2002). Since September 2002, he has been with the National Chiao Tung University, Hsinchu, Taiwan, as a member of the faculty at the Institute of Electro-Optical Engineering. He has authored or coauthored over 60 publications. His current research interests include the epitaxy, design, fabrication, and measurement of high-speed InP- and GaAs-based vertical-cavity surface-emitting lasers, as well as GaN-based lighting-emitting devices and nanostructures.

Yen-Kuang Kuo was born in Chia-Yi, Taiwan, R.O.C., on July 19, 1959. He received the B.S. degree in electrophysics from the National Chiao Tung University, Hsinchu, Taiwan, in 1982, the M.S. degree in electrical engineering from the National Taiwan University, Taipei, Taiwan, in 1984, and the Ph.D. degree in electrical engineering from the University of Southern California (USC), Los Angeles, in 1994.

From 1984 to 1991, he was with the Aeronautical Research Laboratory, Chung Shan Institute of Science and Technology, Taichung, Taiwan. He was a Postdoctoral Research Fellow with the Center for Laser Studies, USC, from 1994 to 1995, where he was engaged in research on passive Q-switching with solid-state saturable absorbers. From 1995 to 1997, he was with the Aerospace Industrial Development Corporation, Taichung. Since 1997, he has been a member of the faculty in the Department of Physics, National Changhua University of Education, Changhua, Taiwan, where he is currently a Professor with the Department of Physics and Institute of Photonics and also the Head of the Laboratory of Lasers and Optical Semiconductors. His current research interests include passive Q-switching with solid-state saturable absorbers and semiconductor materials for light-emitting diodes, organic light-emitting diodes, and semiconductor lasers.

Shing-Chung Wang (M'79–SM'03–LM'07) received the B.S. degree in electrical engineering from the National Taiwan University, Taipei, Taiwan, R.O.C., the M.S. degree in electrical engineering from the National Tohoku University, Sendai, Japan, and the Ph.D. degree in electrical engineering from the Stanford University, Stanford, CA, in 1971.

He has an extensive professional career both in academic and industrial research institutions, which includes as follows: member of the faculty at the National Chiao Tung University, Hsinchu, Taiwan (from 1965 to 1967), Research Associate with Stanford University (from 1971 to 1974), Senior Research Scientist with Xerox Corporation (from 1974 to 1985), and Consulting Scientist with Lockheed-Martin Palo Alto Research Laboratories (from 1985 to 1995). Since 1995, he has been a member of the faculty at the Institute of Electro-Optical Engineering, National Chiao Tung University. He has authored or coauthored over 160 publications. His current research interests include semiconductor lasers, vertical-cavity surface-emitting lasers, blue and UV lasers, quantum-confined optoelectronic structures, optoelectronic materials, diode-pumped lasers, and semiconductor-laser applications.

Prof. Wang is a fellow of the Optical Society of America and the recipient of the Outstanding Scholar Award from the Foundation for the Advancement of Outstanding Scholarship.